Inorg. Chem. **2007**, *46*, 7075–7086

A Computational Study of O–O Bond Formation Catalyzed by Mono- and Bis-Mn^{IV}–Corrole Complexes

Timofei Privalov,*,† Licheng Sun,† Björn Åkermark,‡ Jianhui Liu,§ Yan Gao,§ and Mei Wang§

Organic Chemistry, KTH Chemical Science and Engineering, 10044 Stockholm, Sweden, Department of Organic Chemistry, Arrhenius Laboratories, Stockholm University, 10691 Stockholm, Sweden, and State Key Laboratory of Fine Chemicals, DUT-KTH Joint Education and Research Center on Molecular Devices, Dalian University of Technology (DUT), 116012 Dalian, China

Received May 15, 2007

A detailed computational study of O–O bond formation, catalyzed by monomeric and dimeric Mn–corrole complexes, is reported. The model explicitly takes into account the solvent, with respect to the first and second coordination spheres, while the bulk solvent is described by the polarizable continuum model. Two reaction mechanisms are proposed and computationally characterized: the concerted and the two-step mechanisms. The concerted mechanism is based on a OH^-–$Mn^{IV}O$ interaction via the outer-sphere pathway involving the bridging solvent molecules in the first coordinating sphere. The two-step mechanism is proposed to operate via the coordination of a hydroxide to the Mn^{IV} ion, forming a $MnO(OH)^-$–corrole complex with a strongly nonplanar corrole ligand. Comparison of the proposed mechanisms with available experimental data is performed.

1. Introduction

In natural photosynthesis, water is oxidized in photosystem II (PS II) to molecular oxygen, releasing protons and electrons to sustain all life forms on the earth. This reaction is driven by solar light and occurs in the oxygen-evolving complex (OEC) of PS II through proton-coupled photoinduced electron-transfer processes (see refs 1 and 2 and references therein). The OEC contains a Mn_4Ca cluster, and its chemical structure has been intensively studied in the past decade by different techniques, such as EPR, X-ray crystallography, XANES, EXAFS, etc. (see ref 3). Very recent studies show that the Mn_4Ca cluster probably has a Mn_3CaO_4 twisted-cuboidal structural motif and a fourth dangling Mn bridged with a di-μ-oxo group.[4] During the water oxidation process, the Mn_4Ca cluster passes through five different oxidation states (from S0 to S4, the so-called S cycle) driven by four consecutive photo-oxidation steps.[5] The real active species for the O−O bond formation in OEC is still under debate; however, many agree on the existence of an $Mn^{IV}O$ or $Mn^{V}O$ species in the S4 or S4′ state.

To understand the reaction mechanism of the O−O bond formation in the OEC of PS II and to mimic the water oxidation catalyzed by Mn complexes, several groups have synthesized dinuclear Mn complexes, some of which have shown weak catalytic activity in water oxidation.[1]

We have recently synthesized the mononuclear Mn^{IV} complex **1** and the dinuclear complex **2** with two Mn^{IV}–corrole units connected by a xanthane bridge. We have been able to show that in a basic solution of dichloromethane–acetonitrile containing tetrabutylammonium hydroxide and

* To whom correspondence should be addressed. E-mail: priti@kth.se.
† KTH Chemical Science and Engineering.
‡ Arrhenius Laboratories, Stockholm University.
§ Dalian University of Technology.

(1) McEvoy, J. P.; Brudvig, G. W. *Chem. Rev.* **2006**, *106*, 4455−4483.
(2) (a) Steen, E.; Wondimagegn, T.; Ghosh, A. *J. Inorg. Biochem.* **2002**, *88*, 113−118. (b) Zhang, R.; Harischandra, N.; Newcomb, M. *Chem.−Eur. J.* **2005**, *11*, 5713−5720. (c) Golubkov, G.; Bendix, J.; Gray, H. B.; Mahammed, A.; Goldberg, I.; DiBilio, A. J.; Gross, Z. *Angew. Chem., Int. Ed.* **2001**, *40*, 2132−2134. (d) Steen, E.; Wondimagegn, T.; Ghosh, A. *J. Phys. Chem. B* **2001**, *105*, 11406−11413. (e) van Oort, B.; Tangen, E.; Ghosh, A. *Eur. J. Inorg. Chem.* **2004**, 2442−2445. (f) Gross, Z.; Golubkov, G.; Simkhovich, L. *Angew. Chem.* **2000**, *112*, 4211−4213.
(3) (a) Zouni, A.; Witt, H. T.; Kern, J.; Fromme, P.; Krauss, N.; Saenger, W. Orth, P. *Nature* **2001**, *409*, 739−743. (b) Ferreira, K. N.; Iverson, T. M.; Mhaghlaoui, K.; Barber, J.; Iwata, S. *Science* **2004**, *303*, 1831. (c) Loll, B.; Kern, J.; Saenger, W.; Zouni, A.; Biesiadka, J. *Nature* **2005**, *438*, 1040.
(4) Yano, J.; Kern, J.; Sauer, K.; Latimer, M. J.; Pushkar, Y.; Biesiadka, J.; Loll, B.; Saenger, W.; Messinger, J.; Zouni, A.; Yachandra, V. K. *Science* **2006**, *314*, 821−825.
(5) (a) Haumann, M.; Liebisch, P.; Muller, C.; Barra, M.; Grabolle, M.; Dau, H. *Science* **2005**, *310*, 1019. (b) Penner-Hahn, J. E.; Yocum, C. F. *Science* **2006**, *312*, 1470. (c) Dau, H.; Haumann, M. *Science* **2006**, *312*, 1471. (d) Junge, W.; Clausen, J. *Science* **2006**, *312*, 1470.

10.1021/ic700940x CCC: $37.00
Published on Web 07/28/2007

Scheme 1. The Chemical Structure of Manganese−Corrole Complexes[a]

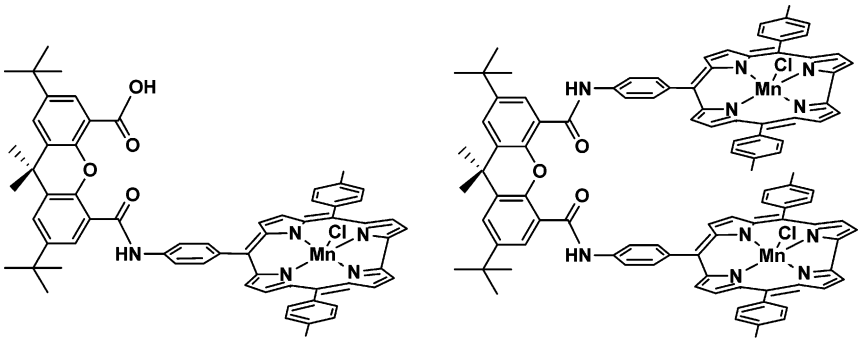

1 **2**

[a] Under the basic conditions, complexes **1** and **2** most likely exist as MnO−corrole active species.

water, both complexes catalyze the formation of molecular oxygen by electrochemical oxidation, complex **2** being by far the most active catalyst of the two.[6] Under the same conditions, the closely related copper^{III} complexes showed no catalytic activity for water oxidation. Under the basic conditions, complexes **1** and **2** most likely exist as MnO−corrole active species (Scheme 1).

Recent theoretical studies,[7,8] demonstrating that intimate details of complex reaction mechanisms can be well-treated with computational methods, encouraged us to employ the well-established density functional theory (DFT) approach. To shed some light on the mechanism for the catalytic activity of the complexes **1** and **2**, we now present an extensive quantum-chemical study of the interaction between these complexes and water and hydroxide.

The oxidation of water in biomimetic models of an OEC typically consists of two major steps, as schematically described by eqs 1 and 2. In the first step, water reacts with the MnO−corrole to form a coordinated hydroperoxyl ion, HOO^-. This reaction could proceed in either a concerted, coupled water deprotonation and $MnOOH^-$ formation or by reaction with hydroxide, first formed by base-promoted deprotonation of the water. In a second two-electron oxidation, molecular oxygen is then formed (eq 2).

$$\{MnO\}_{corrole} + H_2O + X \rightarrow \{MnOO{-}H\}_{corrole} + HX \quad (1)$$

where X = imidazole, pyridine.

$$\{MnOO{-}H\}_{corrole} \rightarrow O_2 + H^+ \quad (2)$$

Alternatively, water or hydroxide could first coordinate to the MnO species. The amount of hydroxide that is readily available for coordination is dependent on the pH of solution and on the strength of a base that is employed in a particular experimental setup. It is also plausible that the coordination of water could coincide with proton transfer, the step that is strongly dependent on particular reaction conditions. Assuming that either one or both mechanisms operate, the O−O bond would then be formed by reductive elimination to give intermediate $MnOOH^-$ species (eq 3).

$$\{MnO\}_{corrole} + HO^- \rightarrow \{MnO(OH)^-\}_{corrole} \rightarrow \{MnOO{-}H\}_{corrole} \quad (3)$$

To provide the first insight into O−O bond formation by Mn−corrole complexes **1** and **2**, we will focus on modeling of eqs 1 and 3, using preformed hydroxide as the nucleophile under the basic conditions. Although hydroxide is a high-energy intermediate, this comparison will indicate the preferred pathway, 1 or 3. The precursor formation, i.e., whether water or hydroxide coordinates to MnO−corrole and whether or not this process is assisted by a simultaneous proton transfer, will be addressed in a forthcoming study.

2. Results and Discussion

2.1. Comparison of the Electronic Properties and Structures of Isolated and Solvated MnO−Corrole Complexes. To understand the properties of the biscorrole complex, the mononuclear complex was first studied. For our purposes, it is sufficient to determine the spin state of the ground-state electronic configuration of an isolated Mn−O−corrole complex, which was found to be a singlet, and to know the order of the spin states of excited electronic configurations without detailed resolution of the exact electronic configuration(s) within the same given spin state (see Tables S1 and S2, Supporting Information, for an illustration of possible spin states). The electronic configurations of an unsubstituted MnO−corrole and the corresponding porphyrine were investigated earlier by Shaik et al.[9] with the detailed resolution of the electronic configurations of all relevant spin states. It was found that the oxo−manganese complex of corrole, the one of our interest, has a singlet closed-shell ground state with manganese in the oxidation state (V).[10] This is fundamentally different from oxo−manganese porphyrin, which has a high-spin manganese^{IV} ground state. The origin of this was traced to the geometrical

(6) Gao, Y.; Liu, J.; Wang, M.; Na, Y.; Åkermark, B.; Sun, L. *Tetrahedron* **2007**, *63*, 1987−1994.

(7) (a) Siegbahn, P. E. M.; Blomberg, M. R. A. *Chem. Rev.* **2000**, *100*, 421−437. (b) Noodleman, L.; Lovell, T.; Han, W.-G.; Li, J.; Himo, F. *Chem. Rev.* **2004**, *104*, 459. (c) Friesner, R. A.; Guallar, V. *Annu. Rev. Phys. Chem.* **2005**, *56*, 389. (d) Siegbahn, P. E. M. *Chem.−Eur. J.* **2006**, *12*, 9217−9227. (e) Ghosh, A. *J. Biol. Inorg. Chem.* **2006**, *11*, 876−890. Ghosh, A.; Steene, E. *J. Biol. Inorg. Chem.* **2001**, *6* (7), 739−752.

(8) Zierkiewicz, W.; Privalov, T. *Dalton Trans.* **2006**, 1867−1874.

(9) de Visser, S. P.; Ogliaro, F.; Gross, Z.; Shaik, S. *Chem.−Eur. J.* **2001**, *22*, 4954−4960.

differences between the oxo−manganese−corrole and porphyrine complexes: the degree of out-of-plane displacement of the MnO moiety essentially controls the order of spin states of a complex (see details in ref 9). Our calculations of the ground-state electronic configuration of MnO−corrole completely agree with those of Shaik et al.

Remarkably, the differences in the electronic energy between the ground state and the lowest excited states of MnO−corrole are rather small: the total energy difference between these states is less than 8 kcal/mol, with an energy difference between some individual configurations of less than 2−3 kcal/mol (see details in ref 9). Therefore, solvent interactions may be expected to influence the order of the close-lying states. It is interesting to note that the charge distribution in the different corrole spin states (the complexes were optimized in all three relevant spin states individually) are different and that the atomic charge on the oxygen atom in MnO−corrole, obtained from simple Mulliken population analysis, increased with the increase of the spin state (see more about the use of Mulliken population analysis in Computational Details). Thus, the negative charge on the oxygen is about 50% higher in the quintet spin state than in the singlet one. Since water oxidation is the ultimate goal of our studies, we decided to specifically investigate how interaction with water molecules could affect the order of the relevant spin states and also the reaction pathway.

The structures of a MnO−corrole complex with one additional water molecule were therefore optimized for the singlet, triplet, and quintet electronic states (**3**, Figure 1). Electronic energies obtained at the B3LYP/lacvp* level predict the quintet state, that is, Mn^{IV}O^{-}−corrole, to be lower than that of the singlet state, Mn^{V}O−corrole, by about 0.7 kcal/mol. The weak basis-set dependence is worth noting. Indeed, the addition of diffuse basis functions to the basis set, that is, the lacvp*+ level, results in a bit larger energy difference between the quintet and singlet state, about 1.0 kcal/mol, in favor of the high-spin state. The conclusion is that the high-spin state of **3** is stabilized by the presence of a hydrogen bond between MnO and a water molecule, as compared to the same spin state in the isolated MnO−corrole complex. This was confirmed by optimizing the geometries of the singlet, triplet, and quintet electronic states of the MnO−corrole species in a model with a larger number of hydrogen-bonded water molecules (models with 5 and 10 water molecules, see below). These larger solvent models

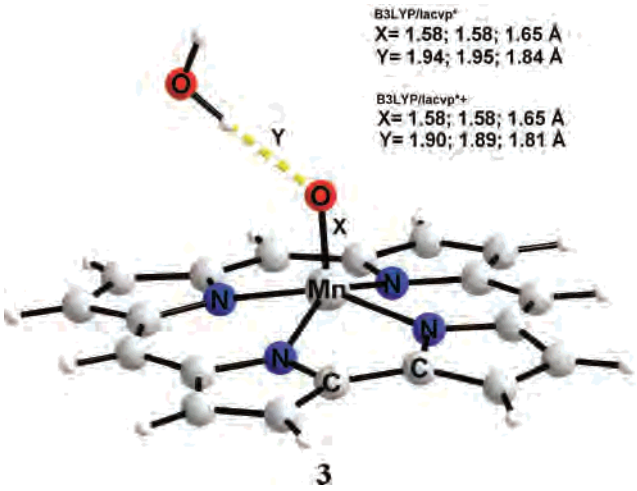

3

Figure 1. Model of MnO−corrole with one water molecule coordinated to an oxygen atom. Labels *X* and *Y* denote MnO and OH distances for singlet, triplet, and quintet electronic spin states, respectively.

predict that the quintet electronic state has the lowest electronic energy at the optimized geometry and that the energy of the optimized singlet electronic state is greater by 1.7 kcal/mol. We attribute the stabilization of **3** in the high-spin state to the increase of the ionic part of the OH bonding with water, which is brought about by an increase of the atomic charge of the oxygen atom from −0.3 (singlet) to −0.46 (quintet), probably due to the increase in dipole−dipole interaction.[11] Accordingly, the OH−O bond is shorter for the quintet electronic spin states, and the bond length follows the order: $Y_{\text{quintet}} < Y_{\text{triplet}} \approx Y_{\text{singlet}}$. The lacvp*+ and the smaller lacvp* basis sets both predict a shortening of the OH−O distance by 0.1 Å in the quintet state and that the Mn^{IV}O^{-} quintet electronic state will be the most-stable one. The MnO and OH−O distances, denoted *X* and *Y*, were investigated for a simple model of MnO−corrole with only one water molecule coordinated to the oxygen atom. They were found to depend on the spin state chosen for the geometry optimization in the following fashion: $X = 1.58$ Å, $Y = 1.94$ Å (singlet); $X = 1.58$ Å, $Y = 1.95$ Å (triplet); $X = 1.65$ Å, $Y = 1.84$ Å (quintet) at B3LYP/lacvp* level. The B3LYP/lacvp*+ level gave $X = 1.58$ Å, $Y = 1.90$ Å (singlet); $X = 1.58$ Å, $Y = 1.89$ Å (triplet); $X = 1.65$ Å, $Y = 1.81$ Å (quintet). Specifically, the quintet state tends to form tighter coordination of water molecules in the first coordination sphere than the singlet and triplet states. This applies also to models with a larger number of explicit solvent molecules.

2.2. Potential Mechanisms for the Formation of the Hydroperoxide Complex MnOOH^{-}. The reaction between hydroxide and MnO−corrole presumably starts with the formation of a MnO−HO^{-}−corrole hydrogen-bonded com-

(10) As explained in ref 9, there are a few formalisms, which enable rationalization of the d-block occupancy. We prefer the formalism where the oxidation state and the charge of the ligand is determined by the number of electrons it "takes" from the metal center to complete its valence shell. That means that water has an oxidation state of 0, the corrole ligand is 3^{-}, and the oxo ligand is 2^{-}, while the oxyl ligand is 1^{-}. For neutral Mn−corrole complexes, Mn atoms appear in the Mn^{III} state and corrole groups appear in the3^{-} state. For an isolated neutral MnO−oxo−corrole complex, Mn may appear as Mn^{IV}, and the corrole then must appear as a cation radical, or Mn appears as Mn^{V} and the corrole has a closed shell. An alternative is to include radical oxyl states. With additional ligands coordinated to MnO−corrole, the distinction between the oxo and oxyl ligands is important and it is done based on Mulliken spin population analysis. For example, some high-spin configurations of MnO−corrole are naturally described by the presence of the O^{-} oxyl ligand (see Table S1, Supporting Information).

(11) In some cases, B3LYP is known to stabilize high-spin states over low-spin states; see, for example: Ghosh, A.; Taylor, P. R. *Curr. Opin. Chem. Biol*. **2003**, *7*, 113−124, due to the effect of the HF exchange term. However, it has also been argued that B3LYP delivers rather consistent performance in a similar complex Mn system; see Lundberg et al., *Inorg. Chem*. **2004**. It is worth also noting that B3LYP works well in differentiating between a fundamentally different singlet ground manganese^{V}−corrole state and a high quintet ground manganese porphyrine spin state; see: de Visser *Chem.—Eur. J*. **2001**.

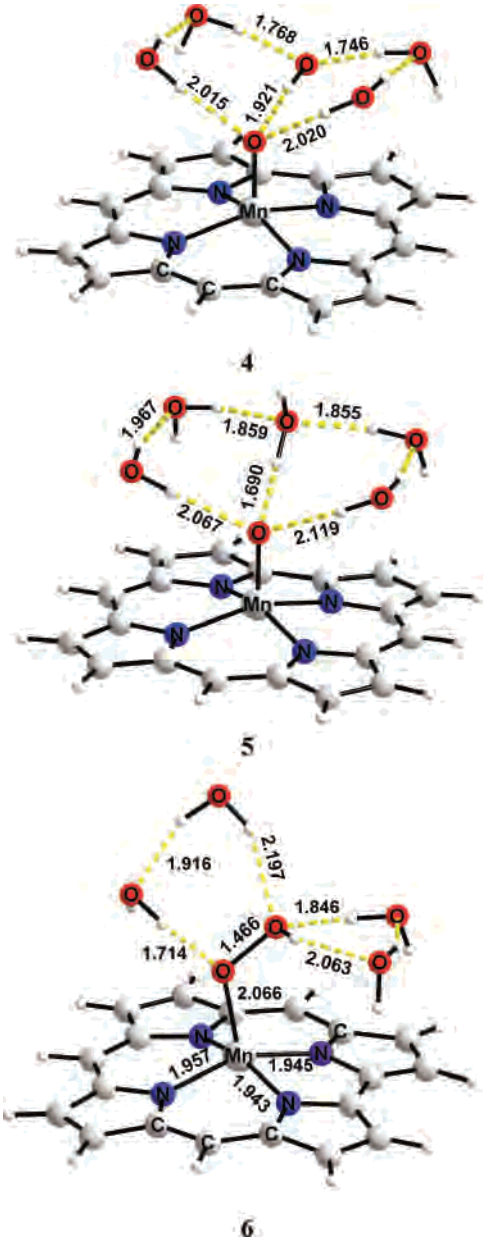

Figure 2. $MnOOH^-$ and MnO complexes with partially filled first coordination sphere. The geometry is optimized for quintet electronic spin states within the B3LYP/lacvp*+ level. All distances are given in angstroms. Additional solvent molecules were added in the reference benchmark calculations. Selected distances: **4**, O−O distance is 2.9 Å; **5**, O−O distance is 2.7 Å.

plex, as described by **5** in Figure 2. This is now a manganese^{III} complex which has a quintet ground spin state. The order of spin states and the vital geometrical parameters are reported in Table S3 (see the Supporting Information).

Realistic models of MnO complexes in protic solvents include explicit solvent molecules in order to describe the bridging of the OH^- and MnO parts of the system (Figure 2). Explicit water molecules seem to be important parts of the model, helping to describe the first coordination sphere and the bridging of the hydroxide ion and MnO−corrole unit. The presence of solvent stabilizes the hydrogen-bonded structures $MnO-HO^-$, similar to **4**, with rather large O−O distances. Complex **4** can be obtained directly by the reaction with hydroxide or by the deprotonation of water, which is hydrogen bonded to the oxo/oxyl atom (compare **4** and **5** in Figure 2). Details of this precursor step (transformation of **5** to **4** possibly with an involvement of a base or a proton-accepting water cluster) will be studied elsewhere. It is worth noting that the comparison of the inner sphere and outer-sphere pathways that we will carry on further is independent of the energetics of the above-mentioned precursor step. This is largely due to the selection of complex **4** as the initial one for both pathways.

Accepting complex **4** as the precursor, it seems that to form the O−O bond, the hydroxide must rotate, with reorientation of the hydrogen-bonded network (conversion of **4** to **6**).

The geometry optimization of a single MnO−corrole unit in the presence of a hydroxide ion, surrounded by a number of water molecules, demonstrates the efficiency of water molecules in creating a network of hydrogen bonds between the hydroxide and the oxyl/oxo atom, which keeps them apart. Thus, *water/hydroxide exchange* and reorganization in the first and second coordination spheres can be expected to be an integral part of the process that leads to the formation of a stable OOH^- group even in the simplified reaction (eq 1) that is an attack of a hydroxide on Mn−oxyl−corrole. The O−O bond of the $MnOOH^-$−corrole unit is described by a well-defined and rather deep potential. This was studied by a relaxed-coordinate scan along the O−O bond as the scan coordinate; each scan point with a particular O−O bond distance was completely energy-minimized with respect to all remaining coordinates except the O−O bond. However, the interaction between the two oxygen atoms will not drive the reaction until the solvent is properly reorganized, which probably proceeds via the formation of intermediates with MnO−HO motifs (complex **4** in Figure 2).

2.3. The Concerted Outer-Sphere Reaction Pathway. There are at least two different reaction pathways to the manganese hydroperoxy complexes $MnOOH^-$. The first one proceeds via the reorganization of the first coordination sphere of the oxyl oxygen atom in the hydroxy complex MnO−HO. Such reorganization is conceived to occur via a concerted transition state that connects the hydrated precursor, MnO−HO, with the successor, MnOOH, along a smooth reaction pathway.

To calculate the energetics of this route, it turns out that it is technically easier to use the reverse search of the concerted outer-sphere transition state starting from the successor, MnOOH, than to perform the direct transition-state search starting from the hydrated precursor, MnO−HO. During the transition state search, the O−O distance was assumed to be the single reaction coordinate, and the relaxed reaction coordinate scan was performed both in the isolated complex, though within the polarizable continuum model (PCM), and in the hydrated MnOOH−corrole complexes, within PCM as well. The performance of the model was tested with the incremental increase of the system up to 12 water molecules explicitly included in the transition-state search. Accurate relaxed-coordinate scans quickly become prohibitively expensive with the increase of the number of solvent molecules. In a model with a large amount of explicit

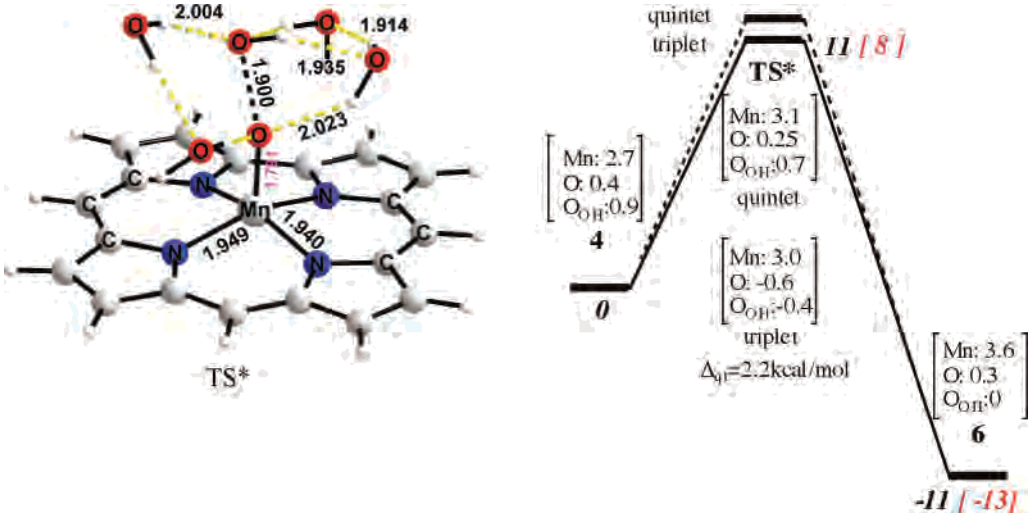

Figure 3. Left: A concerted outer-sphere transition-state structure, obtained by a relaxed-coordinate scan along the reaction coordinate; O−O distance (shown with dashed black line), starting from the successor, the MnOOH complex **4** along the quintet potential surface. The O−O distance was scanned from 1.25 to 3.0 Å in steps of 0.025 Å. This required almost 70 steps, with complete geometry optimization at the B3LYP/lacvp* level at each step. The transition state was further refined, using a lacvp*+ basis set. Right: the energy diagram of the concerted reaction pathway including PCM (black) and "PCM + explicit solvent" (red) electronic energies in kcal/mol. Mulliken spin population analysis is reported for each state. All energies (reported in italic) are in kcal/mol. Δ_{qt} denotes the energy separation between the triplet and quintet-optimized transition states.

solvent molecules, there are many degrees of freedom that correspond to a weakly bound solvent; therefore, a problem of distinguishing local minima on a multidimentional potential surface arises. Thus, one needs to find a compromise between the size of the system and the reliability of optimizing the explicit solvent environment. It was empirically found that models with 4−6 water molecules together with PCM perform well in terms of the accuracy of the optimized structures with respect to the first coordination sphere of MnO and OH$^-$, as well as in terms of computational costs. As a result, the following hydrated transition-state was found (see Figure 3) and confirmed by calculations within PCM-only transition-state search.

The transition-state search was performed with the lacvp* basis set. The optimized transition-state structure was then used to compute the reaction energy at the lacvp*+ basis set, the same basis set that was used to optimize the geometries of the hydrated MnOHO precursor and MnOOH successor. The corresponding electronic activation energy is 8 kcal/mol, while the PCM-only model[12] without additional solvent molecules predicts a higher activation energy of about 11 kcal/mol. The error of the method, which arises from the limited number of water molecules in the first and second coordination spheres, was estimated to be about 3 kcal/mol.

We have found that the triplet spin state is the most-stable electronic configuration at the transition state. However, the quintet transition state is quite close to the stability of the triplet one. The activation energy along the quintet potential surface is only about 2 kcal/mol greater than that for the one with the spin crossing. The reaction path with the quintet−triplet−quintet spin change seems to be spin-forbidden without consideration of spin-orbit coupling (SOC). The transition between electronic states of different spins is allowed due to SOC. The strength of SOC is significant for organometallic complexes because of significant relativistic effects and due to a small energy separation between the different electronic states (see more about SOC and chemical reactivity in ref 13; detailed consideration of the involvement of SOC in the nonadiabatic process of O−O bond formation is currently beyond our scope and will be addressed elsewhere). Mulliken spin population analysis of the lowest electronic state indicates that the manganese ion is in the Mn^{IV} oxidation state, which has three unpaired electrons. The manganese-coordinated oxygen atom and the OH$^-$ group share one additional unpaired electron, antiparallel to the open-shell electrons of the manganese ion. High-spin coupling of the open-shell electrons gives a quintet, at 2.2 kcal/mol above the triplet, which is hardly a significant energy difference. The optimum MnO distance is sensitive to the spin state, which was also obtained for the transition-state geometry search: optimum MnO distances are 1.79, 1.69, and 1.603 Å for the quintet, triplet, and singlet states, respectively. Concluding, the concerted mechanism may operate either along the quintet potential surface or with a spin crossing with a slightly lower activation energy.

2.4. Coordination of OH$^-$ to Manganese: A Two-Step Reaction Pathway. We have seen that the first and the second solvent coordination spheres of hydroxide and MnO are important parts of the molecular structure of both the precursor and the successor.

A first computational model was used with the omission of the explicit solvent molecules in order to simplify the transition-state search. This allows a relatively straightforward gas-phase search of all relevant transition states and a

(12) A pure gas-phase transition-state search was not reliable, we think because electrostatic interactions that arise with changes in the orientation of OH$^-$ with respect to MnO−corrole are unbalanced without a polarizable solvent environment. An activation energy obtained only within continuum solvent methodology is an important benchmark, to which the extended, PCM + explicit solvent model is compared in Figure 3.

(13) Harvey, J. N. *Faraday Discuss.* **2004**, *127*, 165−177.

complete characterization of vibrational frequencies and normal vibrational modes. On the basis of the gas-phase[14] optimized and fully characterized geometries of the transition states, the model can be further upgraded to include a large number of explicit solvent molecules within PCM. Naturally, intermediate complexes may be directly optimized with the appropriate amount of explicit solvent molecules. A proposed two-step reaction pathway begins with the precursor complex **7**, which is identical to **4** when the explicit solvent is considered, with a hydroxide group attached to the oxo group via a hydrogen bond (Figure 4).

For this two-step reaction, we have optimized and characterized two transition states, TS1 and TS2, that appear to be responsible for the formation of MnOH and OO bonds, respectively. Both transition states are confirmed to have exactly one imaginary frequency for the appropriate normal mode. Mulliken spin population analysis for each reaction step is shown in Figure 5. The precursor complex, **7**, could be characterized as a Mn^{IV} complex with the unpaired electron shared by the O−HO group. This configuration corresponds to a quintet spin state. The lower spin states were found to have higher electronic energy. The energy difference is rather small, however, and the difference between the quintet and singlet states is only 2 kcal/mol. The first transition state, TS1, describes the formation of the OMn−OH bond. The addition of solvent and the PCM lowers the activation energy with respect to the reference gas-phase value, but the difference is fairly small. The spin population does not change much relative to that of the precursor, still being well-described as predominantly a Mn^{IV} complex. The intermediate with two Mn−O bonds shows increased Mn−N distances, indicating that the distortion of the corrole has increased. This intermediate, **8**, is moderately stable with respect to the precursor and solvent effects are not large, and the inclusion of solvent increased the stability of this intermediate by only 4 kcal/mol. The interesting changes in Mulliken spin population on manganese occur at the second transition state. We have found that the quintet spin state is the most-stable one, with the dominant unpaired spin density localized on the manganese atom. This, together with the shortened O−O distance, suggests that the electron transfer has occurred to the manganese ion, giving rise to a Mn^{III} configuration. Finally, OOH^- is formed, and the corresponding successor complex **9** is well-described as a Mn^{III} complex in which the quintet is the most-stable spin state.

We have located the analogous triplet and singlet electronic spin states of TS1, which are respectively 6 and 8 kcal/mol higher than the optimized TS1 for the quintet electronic state. We have also located analogues of TS2 for the triplet and singlet electronic states, which are above the quintet state by 3.0 and 7.3 kcal/mol, respectively.

(14) The gas-phase transition-state search worked well, we believe, since the coordination of the hydroxide ion directly to the metal ion takes place, which is probably due to the cancellation of errors in describing the weakening MnO−HO and appearing HO−Mn bonds at the transition state (see TS1). To check this, the continuum solvent model was employed and relative energies were in agreement with the gas-phase data.

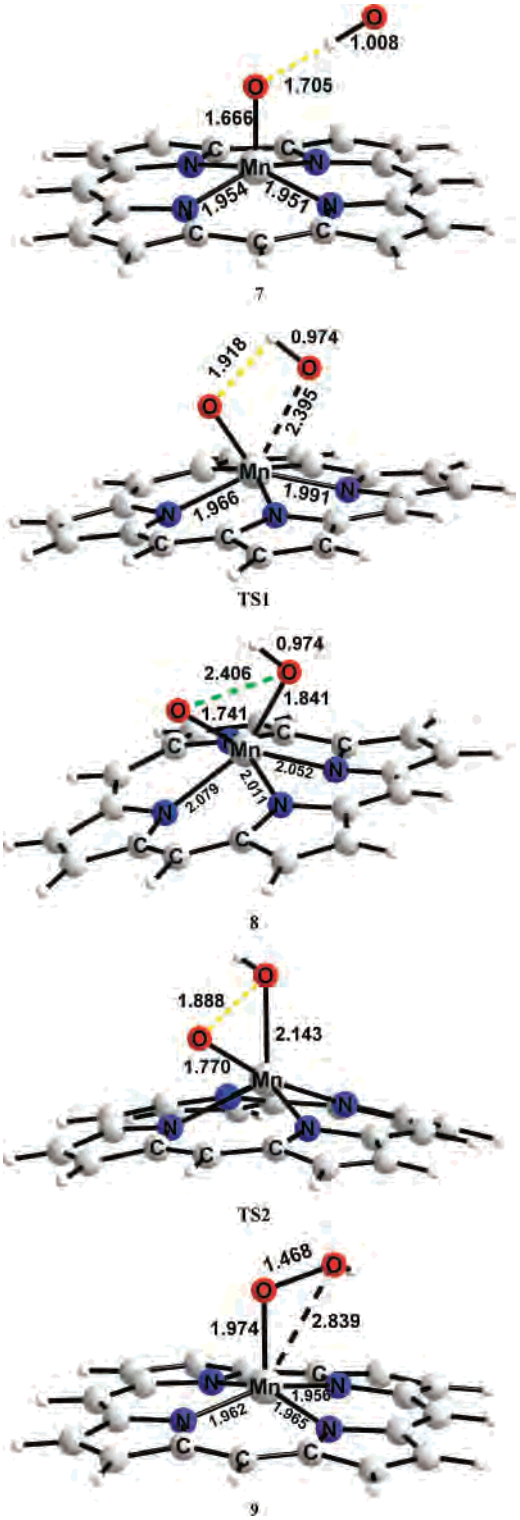

Figure 4. All intermediates and two transition states along the proposed two-step reaction pathway: **7** → TS1 → **8** → TS2 → **9** (see Figure 5 for the energy diagram). All structures are optimized at the B3LYP/lacvp* level. TS1 and TS2 have exactly one imaginary frequency along the appropriate normal mode (quintet spin state). All distances are in angstroms. Additional water molecules are removed for clarity of the presentation (with solvent, complex **7** is identical to complex **4**). TS1: O−O distance is 2.211 Å; MnO distance is 1.70 Å.

Our current understanding of the two-step reaction mechanisms, supported by Mulliken spin populations and optimized transition-state structures for all spin configurations,

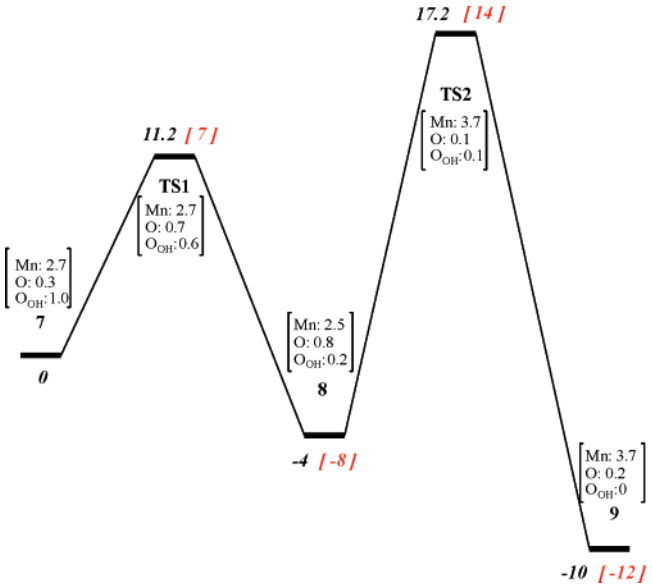

Figure 5. Complete two-step reaction pathway: **7** → TS1 → **8** → TS2 → **9**, along the quintet spin state potential surface, which seems to be the optimal reaction pathway. All energies are reported in italics, energies at the gas-phase level are reported in black (to indicate relative solvent effects only), and PCM reaction energies obtained within the model with small number of explicit solvent molecules are reported in red (the explicit solvent model is the same as that for a concerted mechanism; see Figures 2 and 3). All reaction steps are labeled according to Figure 4. Mulliken spin population analysis is reported for each reaction step. All reaction energies are in kcal/mol.

is that the reaction (eq 3) follows a quintet state potential surface, with the manganese atom being in the highest possible spin state all the time, which is the quartet state (three unpaired electrons) for Mn^{IV} and the quintet state (four unpaired electrons) for Mn^{III}.

It thus appears that the concerted pathway for the formation of MnOOH$^-$−corrole (Figure 2) is favored over the two-step route, where the energy difference is small for the first step (TS1) and considerably greater for the second one (TS2). It is interesting to note that in a recent extensive study of PS II models, Siegbahn also reaches the conclusion that a process similar to the two-step process discussed here is a high-energy path.[7d]

To generate molecular oxygen, the peroxide then has to disproportionate to oxygen and water. Alternatively, a second MnO−corrole unit has to act as oxidant according to eq 2. Dimeric face-to-face biscorrole−MnO complexes can offer the advantage of two close by metal centers, with one acting as catalyst for OOH− formation and another in the final oxygen evolving step.

2.5. Face-to-Face Biscorrole−MnO Complexes: A Sketch of O−O Bond Formation. With the face-to-face biscorrole structure, a third pathway for oxygen formation becomes obvious, direct coupling of the two manganese−oxo groups to form a dimanganese peroxide or a dimanganese oxygen complex. This path is naturally available also to the mono-MnO complexes, which could be capable of forming dimers. However, when the two corrole units are linked by a xanthane bridge as in **2**, dimerization should be favored by the entropy effect. Gas-phase geometry optimizations of the face-to-face biscorrole complexes with and without bridging water molecules identified two possible conformations. In the first one, the distance between Mn ions is only 5.2 Å, presumably due to the interaction between partly overlapping corrole rings. The other one shows the corrole fragments substantially separated from each other, with the Mn−Mn distance of about 10−13 Å. However, the energy difference between those two structures is not large, only 6 kcal/mol, in favor of the structure with the larger Mn−Mn distance.

Geometry optimization shows that the link that holds together the two Mn−corrole fragments is flexible. The biscorrole complex is able to adapt its configuration to accommodate varying number of water molecules. However, bridging of the two manganese ions by one or two water molecules seems to be the preferred coordination (complexes **10** and **11**, Figure 6).

The direct formation of the O−O bond was first studied in the gas phase by bringing together the MnO−corrole units

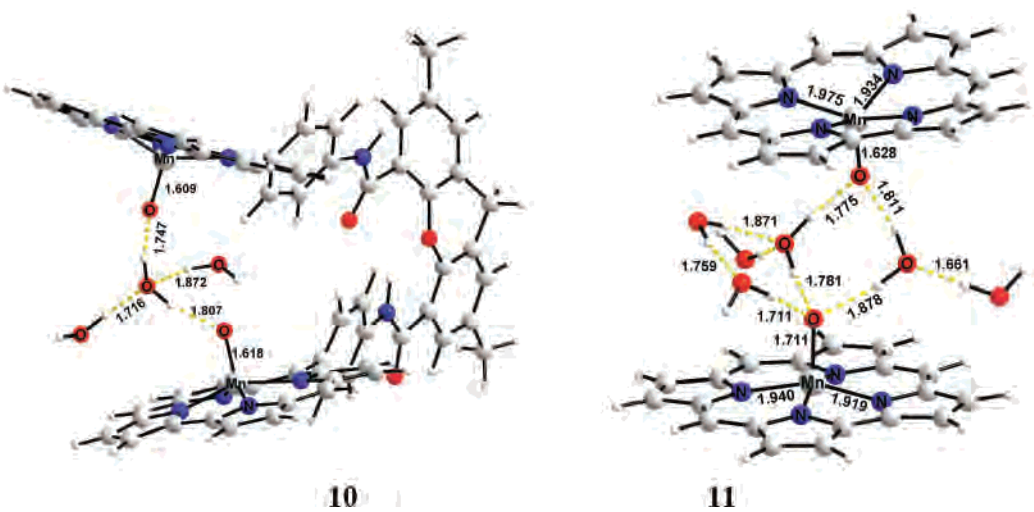

10 **11**

Figure 6. B3LYP/lacvp-optimized structure of the biscorrole−MnO complex, bridged by water molecule(s). **10**: Linked biscorrole−MnO complex; the O−O distance is 4.36 Å, and the Mn−Mn distance is 7.15 Å. **11**: Unlinked biscorrole−MnO complex, bridged by two water molecules with an additional four water molecules between two corroles. The O−O distance is 4.1 Å, and the Mn−Mn distance is 7.0 Å. Yellow dashed lines depict hydrogen bonds.

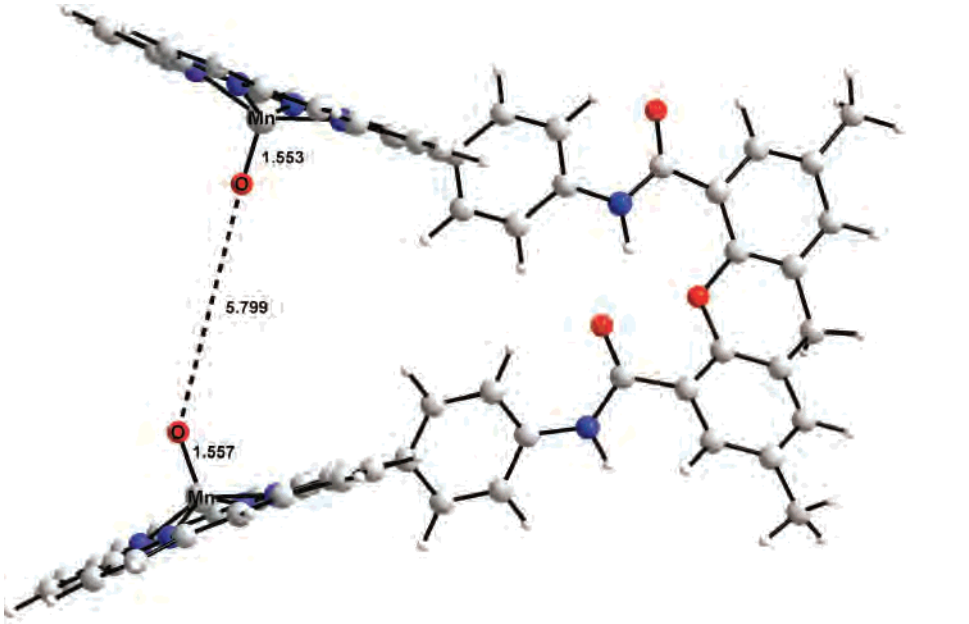

12

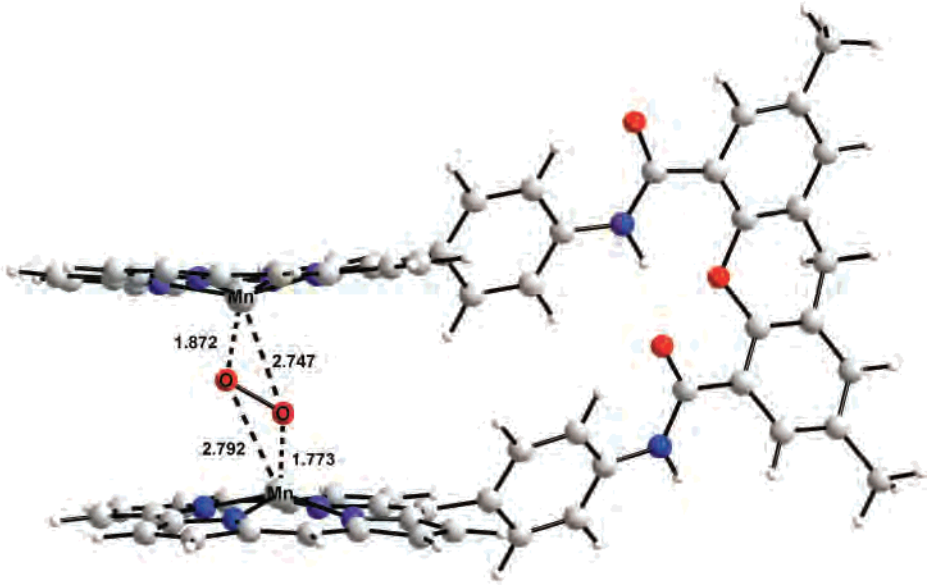

13

Figure 7. B3LYP/lacvp-optimized face-to-face MnO−corrole complexes. **12**: final geometry optimized at the closed-shell singlet electronic spin state. **13**: final geometry optimized at the triplet electronic spin state. All distances are in angstroms.

in a dinuclear complex such as **12**, ending at a Mn−OO−Mn face-to-face biscorrole complex such as **13**, with an evolved O−O bond.

The face-to-face Mn−OO−Mn corrole complex was then optimized at the relevant spin states. It was found that O−O bond was broken for an optimized closed-shell peroxide-like singlet (**12**, Figure 7), while it was preserved for the optimized triplet state structure (**13**, Figure 7). The structure with the broken O−O bond (which is the closed-shell singlet) is more stable than the Mn−OO−Mn complex **13** by about 28 kcal/mol. This means that direct fusion of the O−O bond (going from **12** to **13**) is energetically unfavorable. Furthermore, we found an optimized open-shell singlet analogue of **13** with the intact O−O bond, but this complex was 9 kcal/mol higher in energy than the triplet state. Spin-orbit coupling is very strong in the presence of transition metals; thus, one could expect strong mixing of close electronic spin states, which makes the application of the single-reference DFT method even more complicated.

Due to the size of complexes **12** and **13**, a relatively small basis set, lacvp, was employed for most of our studies. However, we also performed geometry optimization of complex **13** with a much better basis set in the important region on the Mn−O−O−Mn binding motif: we used a lacvp*+ basis set for the O−O pair, a lacvp* basis set for the N atoms within the corrole unit, and a lacvp basis set for the rest of the complex. It turned out that the O−O bond is cleaved in both the closed and open-shell singlet electronic-

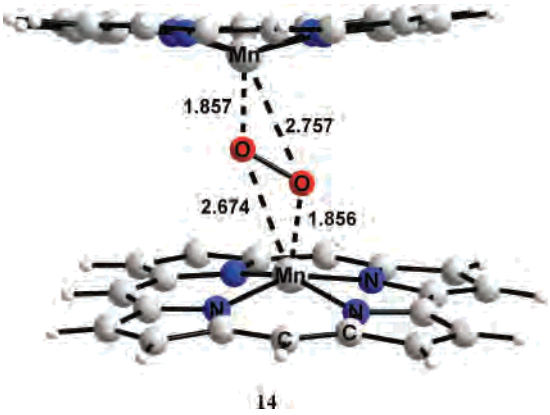

Figure 8. B3LYP/lacvp*-optimized unlinked Mn−OO−Mn biscorrole complex at the triplet electronic spin state. The O−O bond breaks up if the geometry optimization is carried out for the singlet electronic state. The O−O bond length is 1.33 Å. All distances are in angstroms.

state geometry optimizations. The open-shell singlet-state optimization spotted a large area of a quasi-stable O−O bond; the later finally collapses to the Mn−O···O−Mn motif with a cleaved O−O bond in the process of optimization.

In order to obtain a more accurate estimate of the energy difference between the complexes with and without an O−O bond, we performed geometry optimizations of analogues of **13** without the xanthene link. The simplification of the molecular model allowed us to use a larger basis set, lacvp*, for all atoms. No stable Mn−OO−Mn biscorrole geometry could be found at the closed-shell singlet electronic state: the O−O bond dissociates until the basis-set limit is reached. However, a stable analogue of **13**, complex **14** (Figure 8), was reliably found at the triplet spin state. Again, the electronic energy of the dinuclear complex **14** is higher than that of the two isolated MnO−corroles by 19 kcal/mol. Almost the same result, a 21 kcal/mol energy difference, was obtained when an even larger basis set, lacvp**++, was used on both oxygen atoms and the lacvp* basis was used on all remaining atoms. The optimized open-shell singlet state with the uncleaved O−O bond of 1.4 Å appeared almost 10 kcal/mol higher in energy than that of the triplet state. This structure was found to be very sensitive to the quality of the basis set employed for the geometry optimization, with larger basis sets favoring cleaved O−O geometries, which are reached via a large number of optimization steps with a quasi-stable O−O motif. We believe that the deficiency of a single-reference DFT method in describing open-shell low-spin states[15] and the near-degeneracy of electronic levels is the reason for the instability of the open-shell singlet optimization.[16] Interestingly, the optimized O−O bond distance in H_2O_2 at the same level of theory (B3LYP/lacvp*) is 1.46 Å, being close to the one obtained in the open-shell singlet structure, while it is 1.22 Å for an optimized open-shell triplet O_2. The O−O bond distance in an Mn−OO−Mn motif is thus between these two distances. In the optimized open-shell singlet, the O−O motif does not bear any uncoupled spins, while the open-shell electrons of two Mn centers are antiferromagnetically coupled, making it similar to the true peroxide-like structure. It is noteworthy that the structure of the face-to-face Mn−OO−Mn biscorrole part is very similar for linked and unlinked complexes and no appreciable basis-set dependence of the optimized Mn−O distance manifests itself. Comparison of models with linked and unlinked corroles (**13** and **14**, respectively) shows that the formation of the Mn−OO−Mn motif requires some distortion of the link, which is probably the reason why direct O−O bond formation requires slightly more energy for the formation of complex **13** than for **14** (28 kcal/mol versus 19 kcal/mol). Regardless of the difficulties of current DFT methods with open-shell low-spin states, we can reliable establish that there is a strong driving force to cleave the O−O bond (going from complex **13** to complex **12**).

Because the energy difference between two isolated MnO complexes and the coupled dinuclear complex with an O−O bond is so large, one would not expect the solvent environment to stabilize the Mn−OO−Mn motif sufficiently. On the contrary, it is reasonable to assume that solvent interactions will favor an "open" MnO−biscorrole complex such as **12** even more over the O−O coupled dinuclear complex **13** . Spin−orbit effects are expected to mix electronic spin states with high efficiency, which might further favor the cleavage of the O−O bond.

Since the coupling of two manganese−oxo groups seems energetically improbable, a different route to molecular oxygen must be sought. An attractive pathway for oxygen formation is the concerted attack of hydroxide on a Mn−oxo species with the formation of an O−O bond, much like that described for the mononuclear complexes **4** and **6** (see Figure 2), but where the two oxo groups cooperate via a hydrogen-bonded network of water molecules. This is illustrated in Figures 6 and 9 (for the bridged dinuclear system) and Figures 6 and 10 (for the combination of two mononuclear systems).

For the bridged complex, the suggested reaction pathway follows the formation of the MnO−HO precursor **15**, supported by hydrogen bonding. This is seen as the direct analogue of complex **7**. Water molecules play an important role in creating a stabilizing network of hydrogen bonds between two MnO−corrole units. Formation of the MnOOH intermediate **16** is the next reaction step, which involves the proton-coupled formation of the O−O bond. This step is probably achieved in a concerted reaction via a transition state, similar to that of the mononuclear complex (Figure 3) involving the reorientation of the OH^- group relative to MnO and interaction with the oxygen atom, connected to the manganese atom.

Proton-coupled electron transfer would then generate a mixed manganese^{III}dioxygen−manganese^{III}hydroxyl complex **17**. Details of this process will be reported elsewhere.

Linked biscorrole manganese complexes are flexible enough to adapt the structure to the changes in the solvent environment, in particular, a variable number of water molecules, which could bridge the inner parts of face-to-

(15) (a) Blomberg, L. M.; Blomberg, M. R. A.; Siegbahn, P. E. M. *J. Inorg. Biochem.* **2005**, *99*, 949−958. (b) Blomberg, M. R. A.; Siegbahn, P. E. M. *J. Comput. Chem.* **2006**, *27*, 1373−1384.

(16) Several higher spin states were located within less than 1kcal/mol from the reference triplet state.

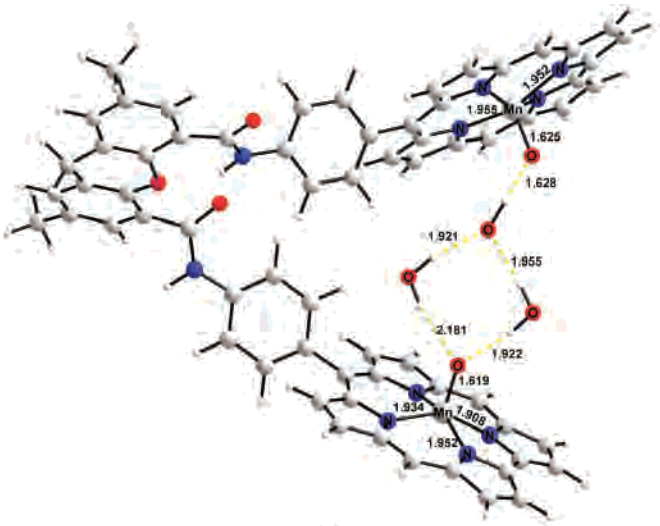

15

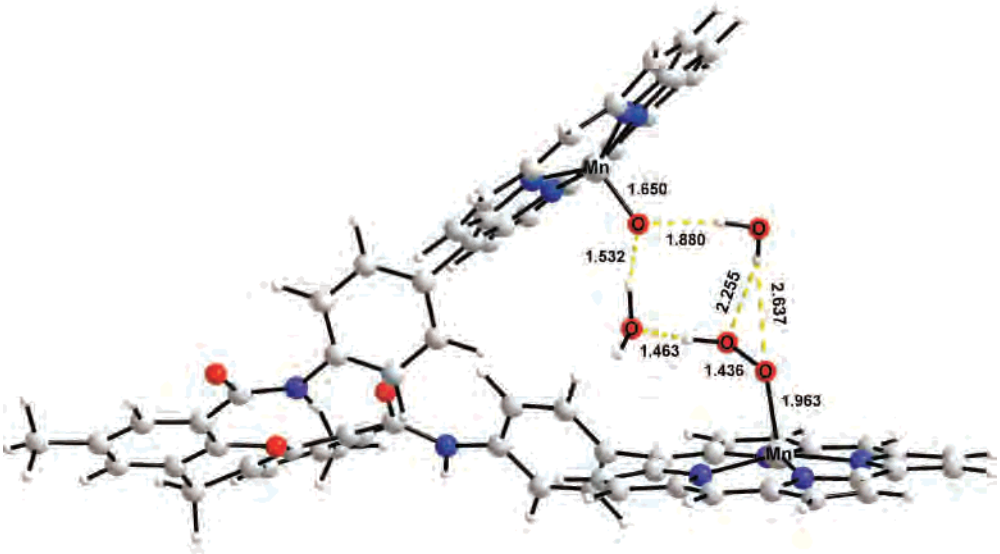

16

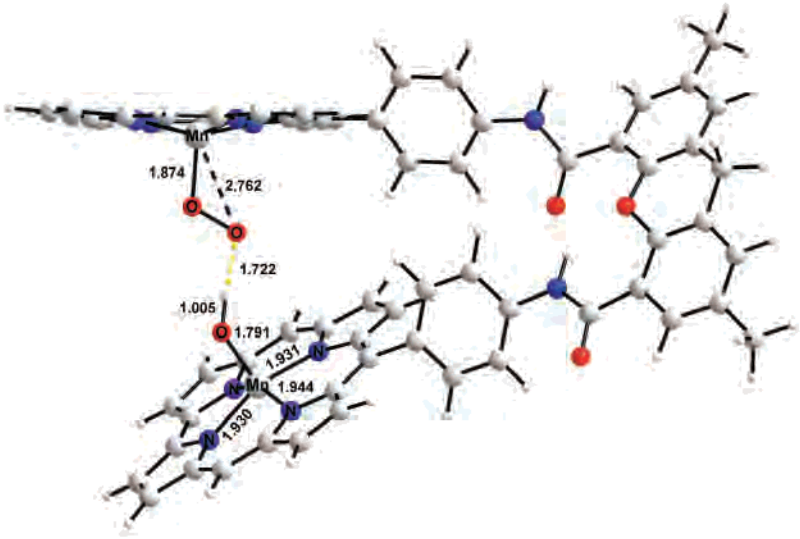

17

Figure 9. B3LYP/lacvp-optimized structures of biscorrole−manganese complexes with one OH^- group. **15**: MnO−HO precursor. **16**: MnO−OH intermediate. **17**: evolved Mn−OO complex. Explicit solvent environment is not shown for clarity of presentation.

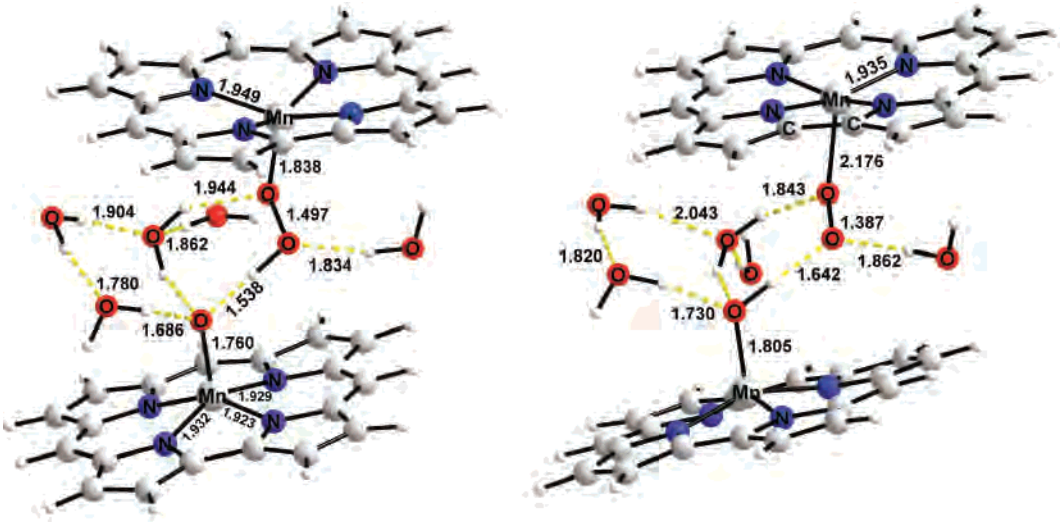

18 19

Figure 10. B3LYP/lacvp-optimized structures of unlinked biscorrole−manganese complexes with OH$^-$ group and additional water molecules. **18**: MnO−OH intermediate. **19**: evolved Mn−OO complex.

face corroles. A simplified model could be derived from the authentic biscorrole complexes: for many purposes, an unlinked MnO−corrole dimer may suffice. An example of such a model is shown in Figure 9. The complex **11** (Figure 6) demonstrates a two-water group bridge between two MnO−corrole units, which is strengthened by extra solvent molecules. A dimeric corrole assembly of this type is surely effective in stabilizing both MnOOH and MnOO motifs (compare to the complexes **18** and **19** in Figure 10). The evolution of molecular oxygen from **18** and **19** is energetically favorable and is expected to be rather effective, considering the mobility of the protons in hydrogen-bonded molecular networks.

3. Conclusion

While the ground state of an isolated monomeric MnO−corrole catalyst is a singlet with a central manganese^V ion, it turns out to become a quintet manganese^{IV} species in a polar-solvent environment. The reason seems to be that a polar solvent stabilizes a Mn^{IV}−oxyl structure relative to the singlet and partly triplet states, which have a predominant, less polar, Mn^{V}oxo structure, though the splittings are quite small. The high-spin configuration is also strongly favored for the Mn^{III}OOH complex, which is obtained by reaction with hydroxide.

For the mononuclear complex, two reaction mechanisms for O−O coupling are proposed and computationally characterized: the concerted and the two-step mechanisms. The concerted mechanism is based on a hydroxide−Mn^{IV}O interaction via the outer-sphere pathway involving the bridging solvent molecules in the first coordinating sphere. The two-step mechanism is proposed to operate via the coordination of a hydroxide to the Mn^{IV} ion, forming a MnO(OH$^-$)−corrole complex with a strongly nonplanar corrole ligand. The actual formation of hydroxide, possibly via an attack of water on MnO−corrole coinciding with a deprotonation step, is not studied per se. However, the omission of this precursor reaction step does not affect our comparison of the inner and outer-sphere mechanisms, because both pathways begin at the same initial complex **4** (or **7**).

By analysis of the potential-energy curves responsible for the formation of the O−O bond in MnO−HO−corrole in a solvent, it is possible to show that the formation of the O−O bond may proceed via a reorganization of the first coordination sphere, including the solvent molecules that bridge MnO and OH$^-$. The calculations suggest that the formation of the OOH$^-$ bond proceeds via a concerted reaction with an activation energy of 8−10 kcal/mol.

The alternative two-step reaction should proceed via the formation of an OMn(OH$^-$)−corrole intermediate. Both transition states along this reaction pathway are characterized: the first one relates to Mn−OH bond formation while the second one is directly related to the formation of an O−O bond. The activation energies for the two-step reaction mechanism are higher than for the one-step, concerted process (see diagram in Figure 5). However, the energy differences are moderate, and one can expect that the reaction in fact proceeds simultaneously via both reaction mechanisms.

The fact that the generation of oxygen is much more efficient in the bridged dinuclear complex **2** than in the mononuclear one **1**[5] suggests that the cooperation of the two corrole units is favorable. The most obvious explanation for this is that the oxygen is formed via the coupling of the two oxo groups to form a dimanganese peroxide, e.g., **12** to **13**. However, this explanation does not hold since, the calculations reliably show that the open structure of **12** is more stable than the coupled structure of **13** by ca. 20 kcal/mol.

A more reasonable explanation is therefore that the O−O bond formation takes place essentially as with the mononuclear complexes, either via a concerted reaction via the direct reaction between one manganese^{IV}oxo group and water or hydroxide or via the coordination of water or hydroxide to manganese, followed by reductive elimination. Because

the linked face-to-face bis(corrole manganese) complexes are flexible, hydroxide and water can easily bridge the two corrole units, forming complexes such as **10** and **15**. The two corrole units can then cooperate in such a way that the O−O bond is formed by a proton-coupled electron-transfer reaction at one MnO unit while the other catalyzes the oxidation of the peroxy group to molecular oxygen.

4. Computational Details

The calculations of the intermediates were performed as follows. First, the geometry optimizations of all intermediate complexes and transition states were carried out using the B3LYP functional[17] with the lacvp*/6-31G(d) basis set.[18,19] All degrees of freedom were optimized. Geometries of each electronic spin state were individually optimized. Mulliken population analysis was employed for the characterization of spin states with the unrestricted DFT method. Open-shell antiferromagnetic electronic states were optimized with the unrestricted DFT method, with appropriate corrections to the energies of open-shell low-spin states applied. The problem of correcting antiferromagnetic low-spin states coupling was not an issue in the present study mainly because high-spin states consistently have lower energy. The correction, as calculated by Siegbahn et al. for the splitting between the parallel and antiparallel spin solution, is about 2 kcal/mol. In the singlet−triplet case the correction value corresponds to twice the calculated energy difference between the triplet and open-shell singlet (see details in ref 20).

Transition states were obtained by utilizing the QST-guided search and were characterized by the presence of exactly one imaginary vibrational frequency along the appropriate normal mode. Relaxed reaction coordinate scans were also employed for finding transition states where appropriate.

It is appropriate to use Mulliken population analysis to obtain atomic spin densities, especially for transition-metal ions (this has been extensively discussed in the literature; see ref 21). The usage of Mulliken charges to estimate partial atomic charges in order to assign formal oxidation states is less reliable but a widely accepted practice. In an open-shell system, the Mulliken spin density is defined as the difference of the Mulliken charges of spin-up and spin-down electrons. The sum over the Mulliken spin densities equals the total spin of the system, but the partial distribution might be basis-set dependent. This was checked, and the Mulliken spin density was stable with respect to the control change of the basis set.

Large face-to-face biscorrole complexes were optimized with the smaller basis set lacvp, to avoid unnecessary computational costs. However, this is of no concern, since the face-to-face mechanistic energy profile is not calculated in the current communication.

In the second step, B3LYP energies of monomeric complexes were evaluated for the optimized geometry using a larger triple-ζ basis set, lacv3p*+/6-311+G(d), with additional diffuse and polarization functions.

When several different basis sets are employed to study particular complex(es) or spin states(s) (see discussion of complexes **12** and **13**), electronic energies are always computed with the same basis set for each and every complex or spin state under consideration. The difference in the electronic energy is that obtained for each basis set separately.

All computations were performed with the *Jaguar* version 6.0 suite of ab initio quantum chemistry programs.[22] Solvent (water) was represented with standard parameters. Gas-phase-optimized structures were used in the solvation calculations within the self-consistent reaction field model as implemented in the *Jaguar* computational package. The solvent was modeled using the self-consistent polarized medium (SCRF/PCM)[23] with additional solvent molecules and/or water molecules in the first and second coordination sphere of the complexes studied.

All frequency analysis was performed with the *Jaguar* version 6.0 program.

Qualitative studies of O−O bond formation by direct fusion in the linked biscorrole complex were performed with the lacvp and lacvp* basis sets. The result was verified in a smaller molecular model with larger basis sets, using the lacvp* and lacvp**++ basis sets for oxygen atoms, while the lacvp* basis set was used for the rest of the system. A large mixed-basis set was employed for the benchmark geometry optimization of the linked biscorrole complex: we used lacvp*+ basis set for the O−O pair, the lacvp* basis set for the N atoms within the corrole unit, and the lacvp basis set for the rest of the complex.

Acknowledgment. This work was supported by grants from The Swedish Energy Agency, the K&A Wallenberg Foundation, and The Swedish Research Council. Computer time via SNAC allocation of computer use at NSC, Linköping, is greatly acknowledged. We are very grateful to Margareta R. A. Blomberg and Per E. M. Siegbahn for discussions of our present work.

Supporting Information Available: Coordinates, structural parameters of optimized complexes, and technical details in a PDF file. This material is available free of charge via the Internet at http://pubs.acs.org.

IC700940X

(17) (a) Becke, A. D. *J. Chem. Phys*. **1993**, *98*, 5648. (b) Lee, C.; Yang, W.; Parr, R. G. *Phys. Rev. B*: *Condens. Matter Mater. Phys*. **1988**, *37*, 785.
(18) Hay, P. J.; Wadt, W. R. *J. Chem. Phys*. **1985**, *82*, 299.
(19) (a) Hehre, W. J.; Ditchfield, R.; Pople, J. A. *J. Chem. Phys*. **1972**, *56*, 2257. (b) Francl, M. M.; Pietro, W. J.; Hehre, W. J.; Binkley, J. S.; Gordon, M. S.; Defrees, D. J.; Pople, J. A. *J. Chem. Phys*. **1982**, *77*, 3654. (c) Hariharan, P. C.; Pople, J. A. *Theor. Chim. Acta* **1973**, *28*, 213.
(20) Noodleman, L.; Case, A. C. *Adv. Inorg. Chem.* **1992**, *38*, 423−470.
(21) Siegbahn, P. E. M. *Curr. Opin. Chem. Biol*. **2002**, *6*, 227.
(22) *Jaguar*, version 6.0; Schrödinger, LLC: Portland, OR, 2005.
(23) The *Jaguar* 6.0 package treats solvated molecular systems with the SCRF method, using its own Poisson−Boltzmann solver, which makes it possible to compute energies in solvent and minimum-energy solvated structures of solvated transition states. For details, see: (a) Tannor, D. J.; Marten, B.; Murphy, R.; Friesner, R. A.; Sitkoff, D.; Nicholls, A.; Ringnalda, M.; Goddard, W. A., III; Honig, B. *J. Am. Chem. Soc*. **1994**, *116*, 11875. (b) Marten, B.; Kim, K.; Cortis, C.; Friesner, R. A.; Murphy, R. B.; Ringnalda, M. N.; Sitkoff, D.; Honig, B. *J. Phys. Chem.* **1996**, *100*, 11775. (c) Cramer, C. J.; Truhlar, D. G. *Chem. Rev.* **1999**, *99*, 2161−2200.